# Neutron pair and proton pair transfer reactions between identical cores in the sulfur region

Michel C. Mermaz
*Commissariat à l'Energie Atomique, Service de Physique Nucléaire, Centre d'études de Saclay, 91191 Gif sur Yvette, Cedex, France*

Michel Girod
*Commissariat à l'Energie Atomique, Service de Physique et Techniques Nucléaires, Boîte Postale 12, 91680 Bruyères-le-Châtel, France*
(Received 1 December 1995)

Optical model and exact finite range distorted-wave Born approximation analyses were performed on neutron pair exchange between identical cores for $^{32}$S and $^{34}$S nuclei and on proton pair exchange between identical cores for $^{30}$Si and $^{32}$S. The extracted spectroscopic factors were compared with theoretical ones deduced from Hartree-Fock calculations on these pairs of nuclei. The enhancement of the experimental cross sections with respect to the theoretical ones strongly suggests evidence for a nuclear Josephson effect.

PACS number(s): 21.10.Jx, 21.60.Jz, 24.10.Ht, 27.30.+t

## I. INTRODUCTION

With regard to angular distribution shape, two neutron transfer reactions between identical colliding cores have been successfully analyzed on the basis of the phenomenological diffractional model [1] for the $^{32}$S($^{34}$S,$^{32}$S) elastic scattering reaction measured at 97 MeV incident energy [2]. In this article, we present a standard optical model analysis and an exact finite range distorted-wave Born approximation (EFR-DWBA) analysis of such a reaction in order to investigate a possible nuclear Josephson effect for the neutron pair transfer reaction in the vicinity of the Coulomb barrier [3]. The same analysis is also performed for the proton pair exchange between identical colliding cores of the $^{30}$Si($^{32}$S, $^{30}$Si) reaction [2]. We define the nuclear Josephson effect in this paper as the simple enhancement of one identical nucleon pair transfer between cores due to the coherent nature of nuclear states in both nuclei exhibiting Bardeen-Cooper-Schrieffer (BCS) identical nucleon pair wave functions. During the collisions, a time dependent Josephson junction is formed between the two cores, the Coulomb barrier acting as an insulator. This was first pointed out by Gol'danskii and Larkin [4]. This nuclear Josephson effect can persist slightly above the Coulomb barrier [3].

The cross section for such an elastic scattering can be written

$$\sigma(\theta)=|f_{\mathrm{el}}(\theta)+\sqrt{NS_iS_f}f_{\mathrm{DWBA}}(\pi-\theta)|^2 \tag{1}$$

for a zero spin system. Here $f_{\mathrm{el}}(\theta)$ is the usual elastic scattering amplitude given by an optical model analysis while $f_{\mathrm{DWBA}}(\pi-\theta)$ is the direct EFR-DWBA transfer reaction amplitude. The values $S_i$ and $S_f$ are the entrance and exit channel spectroscopic factors and $N$ is a normalization factor equal to 1, if the direct surface transfer reaction model is perfectly suitable. If the incident energy is sufficiently above the Coulomb barrier, the forward angle will be dominated by the elastic scattering while the backward angle cross section will be mainly the direct EFR-DWBA cross section.

## II. SPECTROSCOPIC FACTOR

The spectroscopic amplitude $A_{LSJ}$ for two nucleons coupled to $S=0$ or 1 is given for a 0s relative motion by [5]

$$A_{LSJ}=g\sqrt{(2j_1+1)(2j_2+1)(2L+1)(2S+1)} \times \begin{Bmatrix} l_1 & 1/2 & j_1 \\ l_2 & 1/2 & j_2 \\ L & S & J \end{Bmatrix} \langle n_1,l_1,n_2,l_2|N,l,0,0\rangle. \tag{2}$$

The value of $g$ is equal to 1 if the two nucleons are in the same subshell and otherwise equal to $\sqrt{2}$. The pair of braces is the standard $9j$ Wigner symbol and the bracket $\langle|\rangle$ is the Talmi-Moshinsky coefficient for a 0s relative motion and an $N\,L$ center of mass motion. In our case, for a pair of identical nucleons, protons, or neutrons, the total spin is equal to 0. Furthermore, for the $0^+$ ground state configuration, we have $L=J=0$ and $n_1=n_2$, $l_1=l_2$, $j_1=j_2$.

In the case of the wave function extending over several pure shell model configurations, the pick-up spectroscopic factor $S_i$ is given by

$$S_i=\left|\sum_{nk} V_{nk}A_{LSJ}(nlj)\right|^2, \tag{3}$$

where $V_{nk}$ is the configuration amplitude and $A_{LSJ}$ the corresponding spectroscopic amplitude, while for a stripping reaction, the spectroscopic factor $S_f$ is given by

$$S_f=\left|\sum_{nk} (1-V_{nk})A_{LSJ}(nlj)\right|^2, \tag{4}$$

with the same notation as previously. In the following section is presented the microscopic framework in which the configuration amplitudes $V_{nk}$ are obtained.

 

## III. SPECTROSCOPIC FACTORS FROM THE HARTREE-FOCK-BOGOLIUBOV THEORY AND CONFIGURATION MIXING CALCULATIONS

### A. Theory

The theoretical framework within which are described the nuclear structure of $^{30}$Si and $^{32,34}$S is the generator coordinate method [6].

In the first step, potential energy surfaces (PES's) are built from constrained Hartree-Fock-Bogoliubov (HFB) calculations, i.e., from a minimization of the energy functional [7]

$$\delta\langle\Phi_q|\hat{H}-\lambda_0\hat{Q}_{20}-\lambda_2\hat{Q}_{22}-\lambda_Z\hat{Z}-\lambda_N\hat{N}|\Phi_q\rangle=0.$$

In this equation,

(i) $\Phi_q$ is the quasiparticle (qp) vacuum,

(ii) $\hat{H}$ is the many-body nuclear Hamiltonian $\hat{H}=\Sigma_{i=1}^{A}T_i+1/2\Sigma_{i\neq j}v_{ij}$, where $T_i$ is the kinetic energy of the $i$th nucleon, and $v_{ij}$ the finite range density dependent force of Gogny [8],

(iii) $\hat{Q}_{20}$ and $\hat{Q}_{22}$ are external field operators which generate axial and triaxial quadrupole deformations, respectively, and $\hat{Z}$ and $\hat{N}$ are the proton and neutron numbers, respectively.

Finally, the Lagrange multipliers $\lambda_i$ are determined by the constraints $\langle\Phi_q|\hat{Q}_{2i}|\Phi_q\rangle=q_{2i}$, and $\langle\Phi_q|\hat{Z}(\text{or }\hat{N})|\Phi_q\rangle=Z$ (or $N$).

Once the constrained HFB equations are solved, the potential energy surface is defined as

$$V(q)=\langle\Phi_q|\hat{H}|\Phi_q\rangle, \tag{5}$$

where the notation $q=(q_{20},q_{22})$ is used. Since $q_{20}$ and $q_{22}$ are directly related to the Bohr coordinates $\beta$ and $\gamma$, the potential energy surface (5) may also be expressed as $V(\beta,\gamma)$.

In the second step, the dynamical states (i.e., the ground state and excited levels) are sought as

$$|\Psi\rangle=\int f(q)|\Phi_q\rangle dq,$$

where the superposition amplitude $f(q)$ is the solution of the Griffin, Hill, and Wheeler (GHW) equation [9]

$$\int [H(q,q')-EI(q,q')]f(q')dq'=0. \tag{6}$$

In this equation, $H(q,q')=\langle\Phi_q|\hat{H}|\Phi_{q'}\rangle$ is the nuclear kernel, $I(q,q')=\langle\Phi_q|\Phi_{q'}\rangle$ the overlap kernel, and $E$ the energy.

In the third (and final) step, it is assumed that $I(q,q')$ is a Gaussian shape. Under this so-called Gaussian overlap approximation [6], Eq. (2) can be transformed into a second-order differential equation and expressed in the laboratory system

$$\hat{\mathscr{H}}g(q)=Eg(q),$$

where

$$\hat{\mathscr{H}}=-\frac{\hbar^2}{2}\sum_{i,j}\frac{\partial}{\partial q_i}[M^{-1}(q)]_{ij}\frac{\partial}{\partial q_j}+\mathscr{V}(q) \tag{7}$$

is the collective Hamiltonian, $g(q)$ the Gauss transform of $f(q)$, and $\mathscr{V}(q)$ the potential energy surface corrected for zero-point energy $\Delta V(q)$ [i.e., $\mathscr{V}(q)=\mathscr{V}(q)-\Delta V(q)$]. $\hat{\mathscr{H}}$ is formally identical to the Bohr Hamiltonian considered by Kumar and Baranger [10]:

$$\hat{\mathscr{H}}=\mathscr{V}(\beta_0,\beta_2)+\frac{1}{2}(B_{00}\dot{\beta}_0^2+2B_{02}\dot{\beta}_0\dot{\beta}_2+B_{22}\dot{\beta}_2^2)+\sum_{k=1}^{3}\frac{\langle I_i^2\rangle}{2\mathscr{I}_i}, \tag{8}$$

where the collective variables $\beta_0$ and $\beta_2$ are related to the standard Bohr parameters by $\beta_0=\beta\cos\gamma$, $\beta_2=\beta\sin\gamma$, and to the quadrupole moments by $\sqrt{(\pi/5)}(q_0/r_0^2A^{5/3})$ and $\sqrt{(3\pi/5)}(q_2/r_0^2A^{5/3})$, respectively.

The zero-point energy term as well as the collective masses $B_{ij}$ $(i,j=0,2)$ and moments of inertia $\mathscr{I}_i$ $(i=1,3)$, which completely define the tensor $M_{ij}$, are calculated in the cranking approximation [11]. Let us note that the only ingredient used in our set of calculations is the Gogny force. With it, pairing correlations are handled in a fully microscopic way requiring no additional parameters [8]. The collective Hamiltonian $\hat{\mathscr{H}}$ is parameter free.

TABLE I. Theoretical occupation probabilities $V_{nk}^2$ for $^{30}$Si, $^{32}$S, and $^{34}$S nuclei. For each nucleus, the first column corresponds to $V_{nk}^{2\,\text{dyn}}$ and the second one to $V_{nk}^2$ at the minimum of the PES.

| | $^{30}$Si($p$) | | $^{32}$S($p$) | | $^{32}$S($n$) | | $^{34}$S($n$) | |
|---|---|---|---|---|---|---|---|---|
| | $V_{nk}^{2\,\text{dyn}}$ | $V_{nk}^2$ | $V_{nk}^{2\,\text{dyn}}$ | $V_{nk}^2$ | $V_{nk}^{2\,\text{dyn}}$ | $V_{nk}^2$ | $V_{nk}^{2\,\text{dyn}}$ | $V_{nk}^2$ |
| $1d_{5/2\,-1/2}$ | 0.996 | 1.00 | 0.998 | 1.00 | 0.997 | 1.00 | 0.996 | 1.00 |
| $1d_{5/2\,-3/2}$ | 0.990 | 1.00 | 0.997 | 1.00 | 0.995 | 1.00 | 0.995 | 1.00 |
| $1d_{5/2\,-5/2}$ | 0.891 | 1.00 | 0.992 | 1.00 | 0.987 | 1.00 | 0.990 | 1.00 |
| $2s_{1/2\,-1/2}$ | 0.111 | $0.6\times10^{-4}$ | 0.914 | 1.00 | 0.883 | 1.00 | 0.974 | 1.00 |
| $1d_{3/2\,-1/2}$ | 0.006 | $0.5\times10^{-4}$ | 0.081 | $0.7\times10^{-4}$ | 0.099 | $0.5\times10^{-4}$ | 0.783 | 0.999 |
| $1d_{3/2\,-3/2}$ | 0.002 | $0.4\times10^{-5}$ | 0.003 | $0.2\times10^{-4}$ | 0.008 | $0.2\times10^{-4}$ | 0.167 | $0.7\times10^{-3}$ |

### B. Spectroscopic factor

The lowest eigenvalue of this Hamiltonian is the correlated ground state (g.s.) energy. The higher ones are excitation energies of even-parity rotational-vibrational collective levels. The corresponding eigenvectors, the collective wave functions, are used to calculate the g.s. observable quantities. The quantities we are interested in here are the configuration amplitudes $V_{nk}$. In the HFB framework, these quantities are the occupation probabilities of particle states obtained from the constrained HFB calculations. In first approximation, we can consider that the nucleus is well described by the HFB wave function corresponding to the minimum of the PES. We give below the values of the $V_{nk}^2$ obtained in this way; see Table I. Next a better result may be deduced from mixing the constrained HFB solutions using the GHW formalism. Including these correlations in the g.s. wave function leads to significant changes in the predicted occupation probabilities, which are defined in this framework as

$$V_{nk}^{2\mathrm{dyn}} = \int V_{nk}^2(\beta_0,\beta_2) g_{nk}(\beta_0,\beta_2) d\beta_0 d\beta_2 ,$$

where $g_{nk}(\beta_0,\beta_2)$ is the g.s. collective wave function (see Fig. 1).

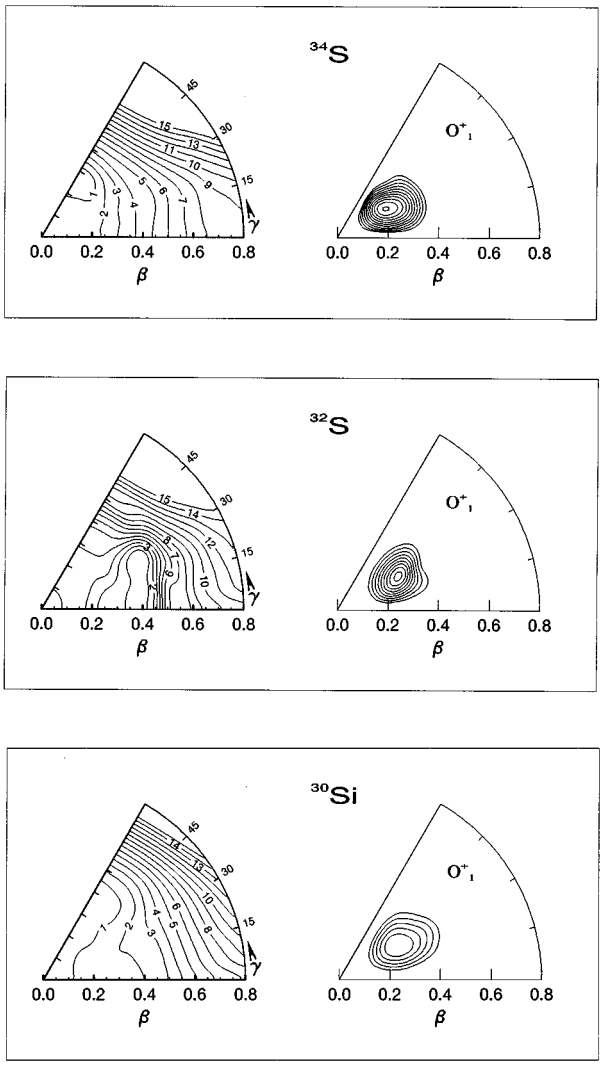


FIG. 1. The potential energy surface for $^{30}$Si and $^{32,34}$S nuclei on the left part, and on the right part, the corresponding ground state collective wave functions.

## IV. HFB RESULTS

### A. Potential energy surfaces

The PES calculations are shown in Fig. 1. At first sight, these three PES's present very different structures. A prolate minimum at large deformation is seen for $^{32}$S while an oblate minimum occurs at small deformation for $^{34}$S. In contrast, no sharp minimum exists for $^{30}$Si. For this last nucleus, it is clear that the wave function corresponding to the minimum of the PES will not be appropriate for the ground state. It is for this nucleus that the effect of the long range correlations is the most important.

### B. Collective levels and transition probabilities

The collective level energies obtained for $^{30}$Si and $^{32,34}$S are shown in Fig. 2. Although here we are only interested in the ground state properties, the rather good agreement obtained for the first collective levels gives some confidence in our calculations. To further check the validity of our collective level predictions, we have calculated reduced transition probabilities for $E2$ transitions. In Table II is shown a comparison between measured [12] and predicted $B(E2)$ values. The good agreement which is obtained suggests that our predictive collective wave functions are also reliable for the calculation of the $V_{nk}$'s.

On one hand, for the pick-up spectroscopic factors, it has turned out in the Hartree-Fock calculations for $^{34}$S nucleus that the $1d_{5/2}$ and the $2s_{1/2}$ neutron shells are completely full while two pairs of neutrons occupy the $1d_{3/2}$ shell. In the same vein for the $^{30}$Si nucleus, it appears that the $1d_{5/2}$ proton shell is also completely full. On the other hand, for the stripping spectroscopic factors, it has turned out in the same calculations that the ground state wave function of $^{34}$S is only the ground state wave function of $^{32}$S coupled to a pair of neutrons in the $1d_{3/2}$ shell. In the same way, the ground

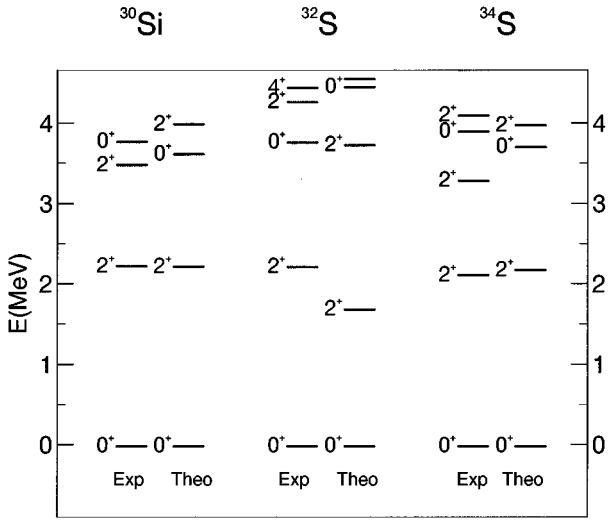


FIG. 2. Experimental and theoretical level scheme of the $^{30}$Si and $^{32,34}$S nuclei for the first even collective states.

TABLE II. Experimental and theoretical transition probabilities $B(E2)$ in $e^2$ b for $^{32}$S, $^{34}$S, and $^{30}$Si nuclei.

| Nucleus | $B(E2)\uparrow$ Expt.[a] | $B(E2)\uparrow$ Theo. |
|---|---|---|
| $^{30}$Si | 0.0215 | 0.0252 |
| $^{32}$S | 0.0300 | 0.0307 |
| $^{34}$S | 0.0212 | 0.0258 |

[a]From the compilation of S. Raman *et al.* [12].

state wave function of $^{32}$S is only the ground state wave function of $^{30}$Si coupled to a pair of protons in the $2s_{1/2}$ shell. Furthermore, it appears in all of these calculations that the $0f$-$1p$ shell is completely empty. Thus the neutron pair transfer as well as the proton pair transfer occur only on the 1*s*-0*d* shell orbitals and consequently the number of nodes of the center of mass motion is then equal to 2.

## V. THE OPTICAL MODEL AND EFR-DWBA ANALYSIS

Figures 3 and 4 present an optical model analysis and EFR-DWBA analysis of the complete elastic scattering plus transfer angular distributions of the $^{32}$S($^{34}$S,$^{32}$S) reaction obtained with the code SATURN-MARS [13]. The optical model elastic scattering parameters which best fit the data at forward angles (angles smaller than 80° c.m.) are given in Table III, families $V1$ and $V2$, and were obtained with the automatic search code PTOLEMY [14]. These parameters correspond to strong absorption using equal geometry for the real and imaginary parts of a Saxon-Woods potential. The phase of the wiggles at backward angles is perfectly reproduced. The agreement is strikingly good at 97 MeV $^{32}$S incident energy. The extracted experimental value of the $NS_iS_f$ spectroscopic factor which best fitted the data points is 1.70 for a theoretical Hartree-Fock value of $S_iS_f = 0.13$. The experimental enhancement factor $N$ is then about 13. In the case of transfer reactions between identical cores, we have in the same figure agreement between the elastic scattering fit at forward angles and the quasielastic transfer reaction cross section at backward angles, leaving no freedom for the adjustment of the optical model parameters. The bound state well parameters are the reduced radius $r = 1.25$ fm and the diffusivity $a = 0.65$ fm. The reduced radius $r$ is already large and favors the transfer reaction quite strongly. The bound state wave functions have two nodes according to the Talmi-Moshinsky transformation. At very backward angles, the experimental points are well above the theoretical fit and correspond to a region of distant collision where the transfer reaction can occur only through Josephson tunneling of Cooper pairs.

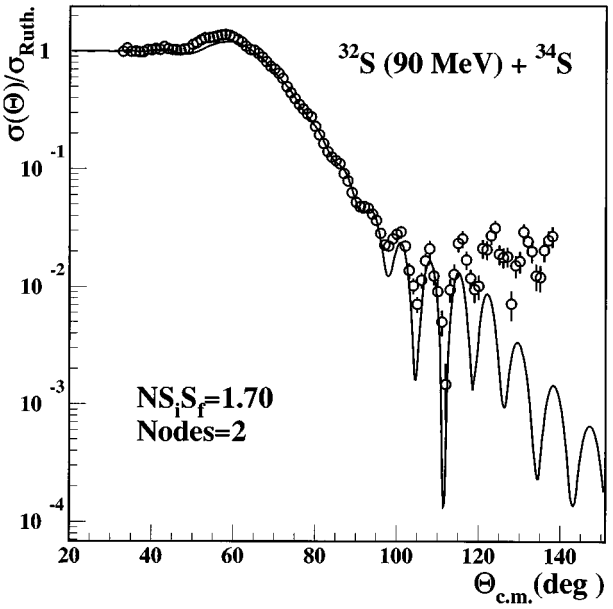


FIG. 3. Angular distribution of the $^{32}$S($^{34}$S,$^{32}$S) elastic scattering plus transfer reaction between identical cores measured at 90 MeV $^{32}$S incident energy. The experimental data points are from the work of J.L. Ferrero *et al.* [2].

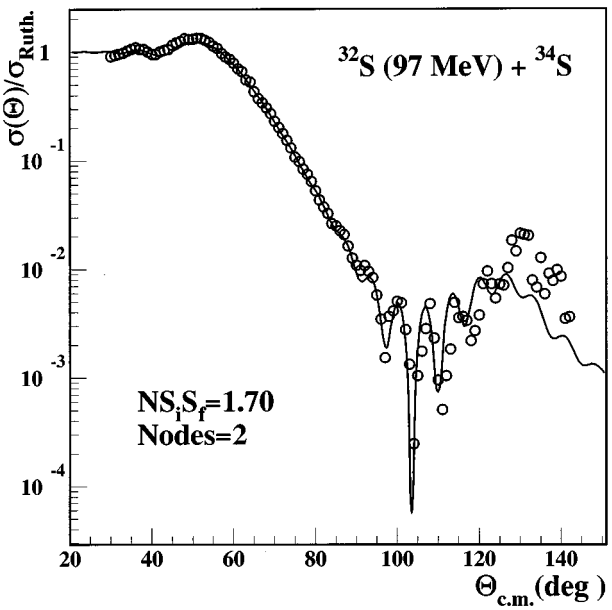


FIG. 4. Angular distribution of the $^{32}$S($^{34}$S,$^{32}$S) elastic scattering plus transfer reaction between identical cores measured at 97 MeV $^{32}$S incident energy. The experimental data points are from the work of J. L. Ferrero *et al.* [2].

TABLE III. Optical model parameter table for $^{32}$S projectile on $^{34}$S and $^{30}$Si target nuclei. The geometry is the same for the real and the imaginary parts. The reduced Coulomb radius $r_c$ is equal to the real part optical model radius $r_0$.

| Target | $^{34}$S | $^{34}$S | $^{30}$Si |
|---|---|---|---|
| $E_{lab}$ (MeV) | 90.0 | 97.0 | 90.0 |
| Potential family | $V1$ | $V2$ | $V3$ |
| $V$ (MeV) | 50.0 | 50.0 | 50.0 |
| $W$ (MeV) | 20.0 | 20.0 | 20.0 |
| $r_0$ (fm) | 1.274 | 1.285 | 1.288 |
| $a_0$ (fm) | 0.517 | 0.495 | 0.494 |

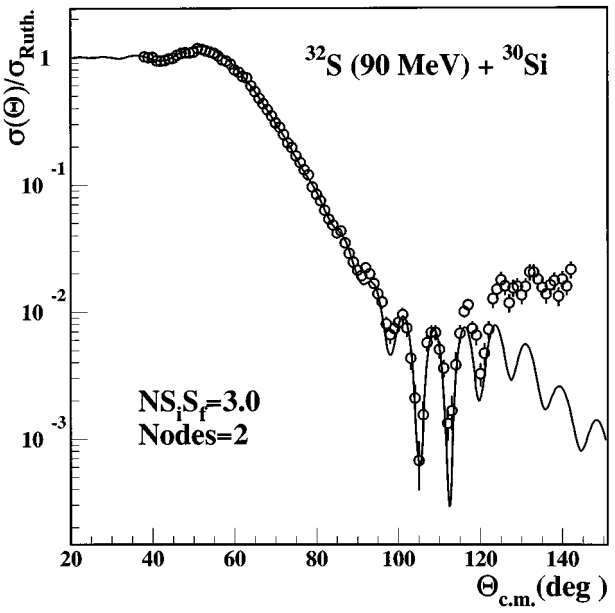


FIG. 5. Angular distribution of the $^{30}$Si($^{32}$S,$^{30}$Si) elastic scattering plus transfer reaction between identical cores measured at 90 MeV $^{32}$S incident energy. The experimental data points are from the work of J. L. Ferrero *et al.* [2].

Figure 5 presents the very same analysis for proton pair transfer reaction between identical cores of $^{30}$Si($^{32}$S,$^{30}$Si). The optical model parameters which best fitted the data points are given in Table III, family *V*3, and correspond to a strong absorption potential. The deviation at very backward angle between the experimental points and the fit can be due to a possible Josephson effect, as already pointed out in the neutron pair transfer reaction case. The extracted experimental value of the $NS_iS_f$ spectroscopic factor is 3.0 for a theoretical Hartree-Fock value of $S_iS_f = 0.23$. We have now an experimental enhancement factor of almost 13.

## VI. DISCUSSION AND CONCLUSION

The unhappiness factor *N* is too high by a factor of 13 for the $^{34}$S,$^{32}$S reaction and too high also by a factor of 13 for the $^{30}$Si, $^{32}$S reaction, which means for both systems that the pair transfer reactions are much too large at backward angles. Let us note that the spectroscopic factors are the largest values which can be obtained for a classical transfer reaction process. The optical model parameters reproduce extremely well the elastic angular distributions at forward angles and also the interference pattern between elastic scattering and transfer processes, in the intermediate angular range for both reactions. This means that the pure transfer reaction is correctly computed and that the deviation from the theoretical absolute values and the disagreement in shape observed at very backward angles might be due to a possible Josephson effect: a current of Cooper pairs between the two colliding cores. This tunneling current of pairs has to be high at very backward angles, where a distant collision occurs due to the Coulomb plus centrifugal barrier playing the role of an insulator layer between the two superconducting fluids. Nevertheless, there is a caveat to this last statement: the unhappiness factor can be larger than 1 in pair transfer reactions, as observed by the authors of Ref. [15] where a factor of 2.3 is encountered for *N* in the $^{74}$Ge($^{18}$O,$^{16}$O)$^{76}$Ge and $^{76}$Ge($^{16}$O,$^{18}$O)$^{74}$Ge reactions due to the possible neglect of sequential processes.

## ACKNOWLEDGMENTS

Sincere thanks are due to Professor B. Bilwes of the University of Louis Pasteur, Strasbourg, for having provided us with her beautiful data on scattering of a $^{32}$S beam $^{28}$Si and on $^{34}$S target nuclei, in tabulated form.

[1] M.C. Mermaz, B. Bilwes, R. Bilwes, and J.L. Ferrero, Phys. Rev. C **27**, 2408 (1983).
[2] J.L. Ferrero, J.A. Ruiz, B. Bilwes, and R. Bilwes, Nucl. Phys. **A510**, 360 (1990).
[3] K. Dietrich, Phys. Lett. **32B**, 428 (1970); Ann. Phys. (N.Y.) **66**, 480 (1971); in *Brazilian Symposium on Theoretical Physics*, edited by E. Ferreira (Livros Tecnicos e Cientificos, Rio de Janeiro, 1975), Vol. 2, p. 213; H. Weiss, Phys. Rev. C **19**, 834 (1979).
[4] V.I. Gol'danskii and A.I. Larkin, Zh Éksp. Teor. Fiz. **53**, 1032 (1967) [Sov. Phys. JETP **26**, 617 (1968)].
[5] P. Bonche (private communication).
[6] P. Ring and P. Schuck, *The Nuclear Many-Body Problem* (Springer, Berlin, 1980), p. 398.
[7] M. Girod and B. Grammaticos, Phys. Rev. C **27**, 2317 (1983).
[8] J. Dechargé and D. Gogny, Phys. Rev. C **21**, 1568 (1980); J. F. Berger, M. Girod, and D. Gogny, Nucl. Phys. **A428**, 23c (1984); **A502**, 85c (1989); Comput. Phys. Commun. **63**, 365 (1991).
[9] D.L. Hill and J.A. Wheeler, Phys. Rev. **89**, 1102 (1953); J. J. Griffin and J.A. Wheeler, Phys. Rev. **108**, 311 (1957).
[10] K. Kumar and M. Baranger, Nucl. Phys. **A110**, 529 (1968); K. Kumar, B. Remaud, P. Auger, J.S. Vaagen, A.C. Rester, R. Foucher, and J.H. Hamilton, Phys. Rev. C **16**, 1235 (1977).
[11] B. Giraud and B. Grammaticos, Nucl. Phys. **A233**, 373 (1974); **A255**, 141 (1975); M. Girod and B. Grammaticos, *ibid.* **A330**, 40 (1979), and references therein.
[12] S. Raman, C.H. Malarkey, W.T. Milner, C.W. Nestor, Jr., and P.H. Stelson, At. Data Nucl. Data Tables **36**, 19 (1987).
[13] Saclay modified version, T. Tamura and K.S. Low, Comput. Phys. Commun. **8**, 349 (1974).r
[14] M.H. Macfarlane and S.C. Pieper, Argonne National Laboratory Report No. ANL 76−11, 1978 (unpublished).
[15] M.-C. Lemaire and K.S. Low, Phys. Rev. C **16**, 183 (1977).